Crystal Fields in Er0.2Y0.98 Studied by Neutron Scattering

Rathmann, Ole Steen; Als-Nielsen, Jens Aage; Bak, Poul Erik; Høg, J.; Touborg, P.

Published in:
Physical Review B

Link to article, DOI:
10.1103/PhysRevB.10.3983

Publication date:
1974

Document Version
Publisher's PDF, also known as Version of record

Crystal fields in $Er_{0.02}Y_{0.98}$ studied by neutron scattering

0. Rathmann, J. Als-Nielsen, and P. Bak
Atomic Energy Commission Research Establishment Risø, 4000 Roskilde, Denmark

J. Høg and P. Touborg
Department of Electrophysics, Technical University, 2800 Lyngby, Denmark

(Received 22 April 1974)

The splitting of the $J = 15/2$ multiplet of Er in an hcp crystal field has been determined by inelastic neutron scattering from a single crystal of $Er_{0.02}Y_{0.98}$. Least-squares fits to the spectra gave crystal-field parameters $B_{20} = -0.34 \pm 0.04$, $B_{40} = (0.7 \pm 0.2) \times 10^{-3}$, $B_{60} = (0.21 \pm 0.02) \times 10^{-4}$, and $B_{66} = (-0.30 \pm 0.03) \times 10^{-3}$ in K, in good agreement with results from bulk magnetization data. A significant line broadening of 1.0 meV full width at half-maximum was clearly observed in the first excited state at 2.2 meV.

INTRODUCTION

The dominant interactions which determine the magnetism of rare-earth metals and their alloys[1] are the indirect exchange interaction and the crystalline field. In addition, the coupling between the magnetic ions and the lattice often plays an important role. In order to separate out the crystal-field interaction for a systematic study Touborg and Høg[2] have investigated a number of rare-earth ions diluted in the nonmagnetic metals Y, Lu, and Sc, which all have the hcp structure of the magnetic heavy rare earths. From magnetization measurements they deduced the parameters B_{lm} in the single-ion crystal-field Hamiltonian

$$H_{cf} = B_{20}\hat{O}_{20} + B_{40}\hat{O}_{40} + B_{60}\hat{O}_{60} + B_{66}\hat{O}_{66} \quad , \tag{1}$$

where $\hat{O}_{lm}$ are the usual Stevens operators.[3] They found that the point-charge model is totally inapplicable for calculating the crystal fields in the rare-earth metals. This result, perhaps not surprising in itself, contrasts sharply with the conclusions of systematic inelastic-neutron-scattering studies of the rare-earth pnictides[4] and Al_2 compounds,[5] from which it was deduced that an effective-point-charge model can account quite well for the crystal-field levels in these metallic or semimetallic compounds. Since the results on the dilute rare-earth alloys seem to have considerable significance for our understanding of the origin of crystal fields in metals, we decided to investigate the reliability of the crystal-field parameters derived from the magnetization data by using the direct spectroscopic method of neutron scattering. The results which we present here for a single crystal of 2% Er substitutionally disolved in Y are, to our knowledge, the first which have been obtained by neutron scattering on the crystal-field levels of a dilute alloy.

EXPERIMENTAL RESULTS

A single crystal of 22 g was prepared as described in Ref. 6. The intensity spectrum of scattered neutrons versus the energy transfer $\hbar\omega = E - E'$ obtained on a triple-axis spectrometer with a fixed filtered energy E of 14.4 meV and a constant wave-vector transfer $\vec{\kappa} = \vec{k} - \vec{k}'$ is shown in Fig. 1, top and middle part. In the top part the wave-vector transfer was 1.8 Å^{-1} along the b axis and in the middle part it was 1.8 Å^{-1} along the c axis in the hcp structure. The sample temperature was 5 K, so only elastic scattering or scattering from the crystal-field ground level with energy *loss* could occur. The neutron spectra contained four well-defined peaks. The small statistical errors of the two peaks at 3.8 and 5.1 meV were obtained by repeating this part of the spectrum six times.

The relatively low background level is quite remarkable considering the fact that the concentration of the magnetic ions is only 2%.

The peak around $\hbar\omega = 0$ for $\vec{\kappa}$ along the c axis (ΓA) is predominantly due to nuclear incoherent scattering. For κ along the b axis (ΓM) this elastic peak has increased by 75% due to magnetic transitions within the ground-state level.

From the scattering cross section [Eq. (3a)] to be discussed shortly, it can be seen that the elastic magnetic intensity varies as $\cos^2\psi$, where ψ is the angle between κ and the hexagonal plane. Figure 2 shows the experimental variation with κ and it is concluded that variations in the intensity due to geometrical effects such as those arising from finite sample size in an inhomogeneous beam are small. The peaks at 2.1, 3.8, and 5.1 meV are due to crystal-field transitions from the ground state to the excited states. We measured the peak around 2.1 meV for κ out to 3.2 Å^{-1} along ΓM. The intensity varied approximately as the squared

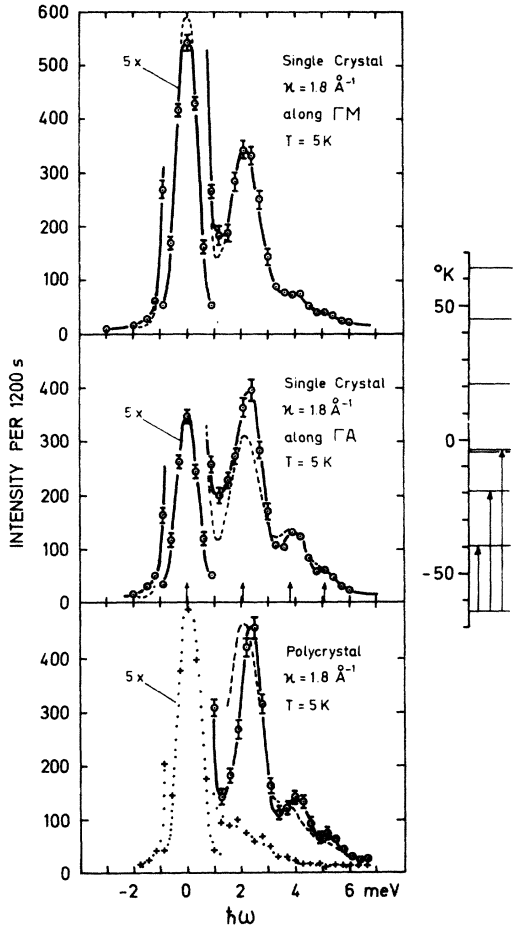

FIG. 1. Inelastic neutron spectra at wave-vector transfer $\vec{\kappa} = 1.8$ Å^{-1}. The upper and middle parts are from a single crystal with $\vec{\kappa}$ along the b axis and c axis, respectively, while the bottom part derives from a polycrystalline sample. The full line is a guide to the eye of the $Er_{0.02}Y_{0.98}$ data. The statistical errors are indicated by error bars where they exceed the size of the circles. In the bottom part, in addition, the scattering from a pure Y polycrystal is shown by crosses with a dotted guide-to-the-eye line. The dashed line is the best simultaneous fit to both single-crystal spectra obtained by diagonalizing Eq. (1) and using a common intrinsic linewidth for all transitions to excited levels. The correction for instrumental resolution effects has been included in this fit.

form factor,[7] demonstrating unambiguously that the scattering is magnetic.

The spectra were also measured at 20 and 50 K. The intensities of all transitions seen at 5 K were observed to decrease due to depopulation of the ground-state level. At the same time a peak at 2.1 meV neutron energy *gain* appeared, originating from transitions from the now populated first excited level to the ground state.

Scattering from lattice vibrations do not contribute to the single-crystal spectra. The momentum-energy-conservation laws determining phonon scattering are not fulfilled anywhere within the spectra if the dispersion relation for pure Y is used,[8] and a few observed phonons propagating in the symmetry directions showed that resonant modes of vibration due to the heavy impurity Er ions do not change the phonon spectrum appreciately from that of pure Y.

In an intermediate stage of its preparation the $Er_{0.02}Y_{0.98}$ sample appeared as a polycrystal. A spectrum from this sample, corresponding to those of the single crystal, is shown in the bottom part of Fig. 1, and the same transitions from the ground level to the excited levels can be identified. For comparison, the scattering from a 25 g pure Y polycrystal at 5 K is also shown. For the polycrystalline material a small phonon contribution is observed around 1–3 meV.

In order to compare the raw spectra with the appropriate scattering cross sections, the instrumental resolution effects must be considered, and the correction for these effects will now be discussed in some detail. With a fixed incident energy in the triple-axis spectrometer, the resolution of the analyzer becomes more and more narrow with increasing $\hbar\omega$, and the observed intensity correspondingly lower. It has been shown by two independent methods[9,10] that the intensity decrease varies as $k'^2/\tan(\theta_A)$, where θ_A is the Bragg angle in the analyzer. Furthermore, the reflectivity of the analyzer crystal, pyrolytic graphite in (002) reflection, varies with $\hbar\omega$[11] and the detector efficiency also varies slightly with $\hbar\omega$. All these factors as well as the factor k'/k, which appears in all in-

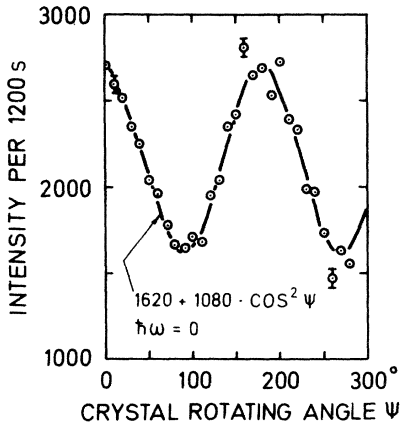

FIG. 2. Neutron scattering intensity from $Er_{0.02}Y_{0.98}$ single crystal at zero energy transfer and at $\kappa = 1.8$ Å^{-1} measured as a function of ψ, the angle between $\vec{\kappa}$ and the hexagonal plane.

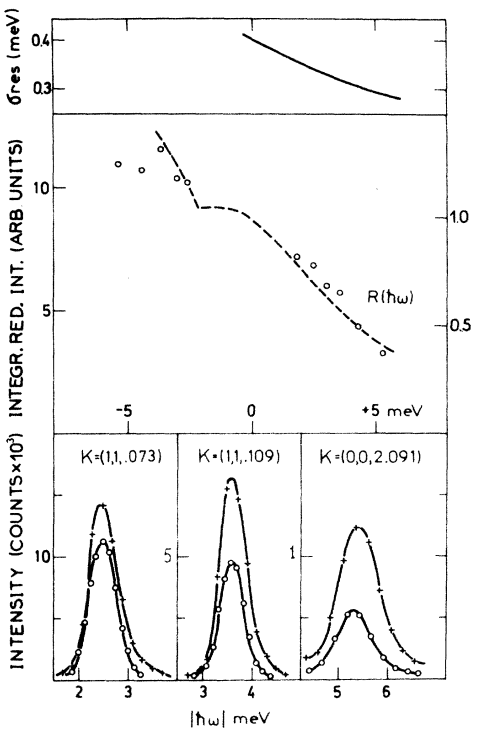

FIG. 3. Bottom: Phonon scattering data used to check the instrumental resolution correction. The scattering vector κ is given in units of the reciprocal lattice. Crosses denote phonon annihilation, open circles phonon creation. Middle: Integrated reduced phonon intensities (see text) compared to the calculated instrumental resolution correction $R(\hbar\omega)$ (right scale). Top: Instrumental resolution width σ_{res}, defined by the resolution function $\exp[-(\hbar\omega)^2/2\sigma_{res}^2]$, vs $\hbar\omega$.

elastic scattering cross sections, are taken into account in a correction factor $R(\hbar\omega)$ normalized to unity at $\hbar\omega = 0$ and shown as the dashed curve in the middle part of Fig. 3. Evidently the variation with $\hbar\omega$ is by no means negligible, so we have checked this variation experimentally by phonon scattering from the same $Er_{0.02}Y_{0.98}$ sample at room temperature. In the bottom part of Fig. 3 are shown the phonon scattering from the annihilation and the creation of two TA phonons (left) and one LA phonon (right) all propagating along the c axis. The phonon cross section is in standard notation[12]:

$$\frac{d^2\sigma}{d\Omega\, dE'} = N\frac{k'}{k} A_2\, \delta(\hbar\omega - E_{ph})\, \delta(\vec{k} - \vec{\tau} - \vec{q}_{ph}) \quad , \tag{2a}$$

with

$$A_2 = b_{coh}^2 \frac{\hbar^2\kappa^2}{2ME_{ph}} [n(E_{ph}) + \tfrac{1}{2} \pm \tfrac{1}{2}]\, e^{-2W(\kappa)} \tag{2b}$$

and

$$n(E_{ph}) = [\exp(E_{ph}/kT) - 1]^{-1} \quad . \tag{2c}$$

In Eq. (2b) the + sign is used for phonon creation, the − sign for annihilation. In the middle part of Fig. 3 are shown the integrated phonon intensities divided by A_2. This quantity is expected to vary as $R(\hbar\omega)$ discussed above, and the agreement in the interval $0 < \hbar\omega < 5$ meV where we apply the resolution correction to the crystal-field spectrum is indeed very good.

ANALYSIS

The $4f$ ground-state multiplet of Er, with $J = \frac{15}{2}$, is split by the crystal field into eight doublets. In accordance with the notation of Marshall and Lovesey,[12] we denote the energies by E_n and the states by $|\Gamma_n v\rangle$, with $n = 0$ as the index for the ground state with $E_0 = 0$. The label v distinguishes between the two degenerated wave functions of each level. The cross section for the transition $\Gamma_0 \to \Gamma_n$ is then

$$\frac{d^2\sigma}{d\Omega\, dE'} = cN\frac{k'}{k} A_1\, T_n\, \delta(\hbar\omega - E_n) \quad , \tag{3a}$$

with

$$A_1 = \left(\frac{1.91e^2}{m_e c^2}\frac{1}{2} g F(\vec{\kappa})\right)^2 e^{-2W(\kappa)} \quad , \tag{3b}$$

and

$$T_n = \sum_{\alpha\beta} (\delta_{\alpha\beta} - \tilde{\kappa}_\alpha \tilde{\kappa}_\beta) \sum_{vv'} P_0 \langle v\Gamma_0 | J_\alpha^* | \Gamma_n v'\rangle \times \langle v'\Gamma_n | J_\beta | \Gamma_0 v\rangle \quad . \tag{3c}$$

N is the total number of atoms, the fraction $c = 0.02$ being Er atoms. The g factor is 1.2 for Er and the remaining symbols in Eq. (3b) have their usual meaning.[12] In the expression for the transition probabilities Eq. (3c), $\tilde{\kappa}_\alpha$ is the Cartesian α component of $\vec{\kappa}/\kappa$, and p_0 is the occupation probability of one of the two ground states. At 5 K, p_0 is near 0.5.

The spectra in Fig. 1, $I_{CF}(\hbar\omega)$, were analyzed by a least-squares fit to the expression

$$I_{CF}(\hbar\omega) = S\left(\sum_n T_n (\sqrt{2\pi}\sigma_n)^{-1} \exp[-(\hbar\omega - E_n)^2/2\sigma_n^2]\right) + \alpha_{ni} \exp[-(\hbar\omega/\sqrt{2}\sigma_0)^2] + B. \tag{4}$$

Here the δ function in Eq. (3a) has been changed to a Gaussian distribution of width σ_n in order to take the instrumental resolution as well as an intrinsic linewidth into account. The width σ_0 for elastic scattering is known from a scan of the incoherent scattering from V, whereas the widths for inelastic transitions contained one adjustable parameter σ, in the expression $\sigma_n^2 = (\sigma^2 + \sigma_{res,n}^2)$, with the resolution width $\sigma_{res,n}$ given in the top part of Fig. 3. The factor $R(\hbar\omega)$ accounts

TABLE I. Crystal-field parameters for Er^{3+} in $Er_{0.02}Y_{0.98}$.

	This experiment	From magnetization data
B_{20} (K)	-0.34 ± 0.04	-0.31 ± 0.03
B_{40} (K)	$(0.7 \pm 0.2)10^{-3}$	$(0.6 \pm 0.3)10^{-3}$
B_{60} (K)	$(0.21 \pm 0.02)10^{-4}$	$(0.24 \pm 0.02)10^{-4}$
B_{66} (K)	$(-0.30 \pm 0.03)10^{-3}$ [a]	$(-0.28 \pm 0.03)10^{-3}$
σ (meV)	0.43 ± 0.05	

[a]The sign is undetermined by the neutron scattering experiment.

for the decreasing instrumental sensitivity as explained above. The nuclear incoherent scattering is accounted for by the fit parameter α_{ni}. The background B was determined by the intensities with $\hbar\omega < -3$ meV and $\hbar\omega > 7$ meV.

The transition probabilities T_n and the energies E_n are determined by the crystal-field parameters B_{20}, B_{40}, B_{60}, and B_{66}. Finally, the scale factor S was also a fitting parameter. The best-fit value of S agreed with the value obtained from the intensity observed with a V sample of similar shape to the $Er_{0.02}Y_{0.98}$ sample.

The calculated spectra obtained in a *simultaneous fit to both* spectra in Fig. 1 are shown as dashed lines in Fig. 1, and the resulting best-fit parameters are given in Table I. The dashed line in the bottom part of Fig. 1 is a powder spectrum calculated from this set of parameters. The small phonon contribution is included in this theoretical spectrum.

The corresponding energy levels are shown in the right part of Fig. 1 and the centers of the transition peaks are indicated by arrows on the energy axis.

The ground-state level, from which the strongly anisotropic magnetic elastic scattering originates, turns out mainly to consist of $|\pm\frac{13}{2}\rangle$ states, while the inelastic peaks in the spectra are due to transitions to three excited levels dominated by $|\pm\frac{11}{2}\rangle$, $|\pm\frac{9}{2}\rangle$, and $|\pm\frac{15}{2}\rangle$, respectively. When $\vec{\kappa}$ is along ΓA the magnetic scattering is caused by matrix elements of J_x and J_y. Hence, the small elastic magnetic scattering, about $\frac{1}{3}$ of the value for $\vec{\kappa}$ along ΓM, is purely due to the small components of other m_J states than $|\pm\frac{13}{2}\rangle$ which are mixed into the ground states via the O_6^6 term of the Hamiltonian in Eq. (1). The transition to the first excited level is nearly isotropic because J_x, J_y, and J_z have matrix elements from the ground level to this level of nearly equal size. The last two transitions in the spectra are caused purely by matrix elements of J_x and J_y. Hence, the intensity ratio between the $\vec{\kappa}$ along-ΓA direction and $\vec{\kappa}$ along-ΓM direction should be exactly 2.

At first sight it may seen surprising that one can deduce four crystal-field parameters with reasonable accuracy and a common lifetime from the upper and middle spectra in Fig. 1. The reason is that the different combinations of matrix elements for $\vec{\kappa}$ along ΓA and $\vec{\kappa}$ along ΓM constrain the possible values of the crystal-field parameters significantly.

It is obviously necessary to include a finite lifetime of the excited states as the width of the peak at 2.1 meV exceeds the experimental resolution by more than 50%. The intrinsic width, which of course cannot be accounted for by the Hamiltonian in Eq. (1), is very likely caused by the exchange interaction between the Er ions. In a 2% alloy there is a 24% chance that an Er ion among its 12 neighbors has another Er ion. If we may crudely assume an Ising-like nearest-neighbor-only exchange coupling $-gJ_z^{(0)}J_z^{(1)}$, it is straightforward by a perturbation calculation to find the corresponding splitting of the degenerate levels in Fig. 1. With $g \sim 0.02$–0.04 meV from the known spin-wave dispersion in pure Er[13,14] we then find a splitting 0.4–0.9 meV, i.e., in the same order of magnitude as the observed widths of the inelastic peaks.

CONCLUSION

We conclude that the crystal-field parameters obtained from the magnetization data[2] for Er diluted in Y are, within the uncertainties of the two experiments, in accordance with those obtained by the more direct spectroscopic method of neutron scattering. This agreement supports the reliability of the crystal-field parameters found in the systematic study of rare-earth (RE) ions in different matrices.[2] On the other hand, it is also clear from Fig. 1 that the excited states of the Er ions are probed in more detail by neutron scattering than the simple Hamiltonian in Eq. (1) can account for. First there is a significant line broadening, even at 5 K, of the excited levels, most clearly seen in the intense transition to the first excited state. Second, the difference between the best-fit curve based on Eq. (1) and the observed intensities is substantially larger than can be explained by the experimental uncertainties. It seems likely that the interaction between the $4f$ and the conduction electrons is responsible for these effects, either by the direct interaction[14] or by the indirect exchange coupling to nearby Er ions.

ACKNOWLEDGMENTS

The authors appreciate fruitful discussions with A. R. Mackintosh and W. F. Brinkman.

[1]*Magnetic Properties of Rare-Earth Metals*, edited by R. J. Elliott (Plenum, New York, 1972).
[2]J. Høg and P. Touborg, Phys. Rev. B 9, 2920 (1974); P. Touborg and J. Høg, Phys. Rev. Lett. (to be published).
[3]K. W. H. Stevens, Proc. Phys. Soc. Lond. A 65, 209 (1952).
[4]R. J. Birgeneau, E. Bucher, J. P. Maita, L. Passell, and K. C. Turberfield, Phys. Rev. B 8, 5345 (1973); K. C. Turberfield, L. Passell, R. J. Birgeneau, and E. Bucher, Phys. Rev. Lett. 25, 752 (1970).
[5]H. G. Purwins, E. Walker, B. Barbara, W. F. Rossignol, and P. Bak, J. Phys. C (to be published).
[6]K. A. McEwen and P. Touborg, J. Phys. F 3, 1903 (1973).
[7]We have used the value of F ($\kappa = 1.8$ Å^{-1}) = 0.9 as measured for Tb by Lander *et al.* [Phys. Rev. B 8, 3237 (1973)].
[8]S. K. Sinha, T. O. Brun, L. D. Muhlestein, and J. Sakurai, Phys. Rev. B 1, 2430 (1970).
[9]H. B. Møller and M. Nielsen in *Instrumentation for Neutron Inelastic Scattering Research* (IAEA, Vienna, 1970), pp. 49–70.
[10]N. Chesser and J. D. Axe, Acta Crystallogr. A 29, 160 (1973).
[11]S. M. Shapiro and N. Chesser, Nucl. Instrum. Methods 101, 183 (1972).
[12]W. Marshall and S. W. Lovesey, *Theory of Thermal Neutron Scattering* (Clarendon, Oxford, 1971).
[13]R. M. Nicklow, N. Wakabayashi, M. K. Wilkinson, and R. E. Reed, Phys. Rev. Lett. 27, 334 (1971).
[14]J. Jensen, J. Phys. F 4, 1065 (1974).